

# The effect of curvature in thawing models

Sergio del Campo\*

*Instituto de Física, Pontificia Universidad Católica de Valparaíso,  
Avenida Brasil 2950, Casilla 4059, Valparaíso, Chile.*

Víctor H. Cárdenas†

*Departamento de Física y Astronomía,  
Universidad de Valparaíso, Gran Bretaña 1111, Valparaíso, Chile*

Ramón Herrera‡

*Instituto de Física, Pontificia Universidad Católica de Valparaíso ,  
Avenida Brasil 2950, Casilla 4059, Valparaíso, Chile.*

## Abstract

We study the evolution of spatial curvature for thawing class of dark energy models. We examine the evolution of the equation of state parameter,  $w_\phi$ , as a function of the scale factor  $a$ , for the case in which the scalar field  $\phi$  evolve in nearly flat scalar potential. We show that all such models provide the corresponding approximate analytical expressions for  $w_\phi(\Omega_\phi, \Omega_k)$  and  $w_\phi(a)$ . We present observational constraints on these models.

PACS numbers:

---

\*Electronic address: [sdelcamp@ucv.cl](mailto:sdelcamp@ucv.cl)

†Electronic address: [victor@dfa.uv.cl](mailto:victor@dfa.uv.cl)

‡Electronic address: [ramon.herrera@ucv.cl](mailto:ramon.herrera@ucv.cl)

## I. INTRODUCTION

About a decade ago, current measurements of redshift and luminosity-distance relations of Type Ia Supernovae (SNe)[1] indicate that the expansion of the universe presents an accelerated phase [2, 3]. In fact, the astronomical measurements showed that Type Ia SNe at a redshift of  $z \sim 0.5$  were systematically fainter which could be attributed to an acceleration of the universe caused by a non-zero vacuum energy density. As this shows a result, that the pressure and the energy density of the universe should violate the strong energy condition,  $\rho_\phi + 3p_\phi > 0$ , where  $\rho_\phi$  and  $p_\phi$  are energy density and pressure of some exotic, unknown and unclustered matter component, dubbed dark energy[4] (see also Refs. [5, 6] for recent reviews). A direct consequence of this, is that the pressure must be negative.

Various models of dark energy have been proposed so far. Perhaps, the most traditional candidate to be considered is a non-vanishing cosmological constant [7, 8]. Other possibilities are quintessence [9, 10], k-essence [11–13], phantom field [14–16], holographic dark energy [17, 18], etc. (see Ref. [19] for model-independent description of the properties of the dark energy and Ref. [20] for possible alternatives).

The first step toward understanding the property of dark energy is to make clear whether it is a simple non-vanishing cosmological constant or its genesis comes from other sources which dynamically change in time. It is possible to distinguish between these two possibilities by taking into account the evolution of the equation of state parameter defined by  $\omega_\phi \equiv p_\phi/\rho_\phi$ .

In what concern to the dynamical dark energy (or quintessence) its physics is described by a scalar field,  $\phi$ , (quintessence scalar field), with canonical momentum[21]. One of the main characteristic of the quintessence field is when it rolls the self interacting potential curve. It will provide a negative pressure if the potential curve is quite flat. In this way, the quintessence scalar field evolves slowly enough to drive the present cosmic acceleration.

Since the evolution of the quintessence scalar field may be described by the change of the equation of state parameter  $w_\phi$ , so that we could distinguish two possible situations: the case in which  $dw_\phi/d\phi < 0$  and  $dw_\phi/d\phi > 0$ . The former case is referred as the freezing and the later the thawing scenarios, respectively[22](see also Ref. [23] for details). While the observational data up to now are not discriminating in the sense that we could not distinguish between a freezing or a thawing phases by the variation of the equation of state parameter,

it is expected that will be able to do so with the next decade high-precision astronomical observations.

On the other hand, in what concern to the curvature of the universe, today we do not know precisely the geometry of the universe, since we do not know the exact amount of matter present in the Universe. Various tests of cosmological models, including spacetime geometry, galaxy peculiar velocities, structure formation and very early universe descriptions (related to the Guths inflationary universe model [24]) support a flat universe scenario. However, by using the seven-year Wilkinson Microwave Anisotropy Probe (WMAP) data combined with measurements of Type Ia SNe and Baryon Acoustic Oscillations (BAO) in the galaxy distribution, it was reported that the value for the curvature density parameter,  $\Omega_k = -0.0057^{+0.0066}_{-0.0068}$  (68% CL) represents a preferred model, which is slightly closed [25, 26].

In this paper we would like to study some of the consequences that this slightly curvature may have on the evolution of the universe, together with the the situation in which the thawing cosmological evolution for the quintessence scalar field is invoked. The outline of the paper goes as follow, in section II we present the model to be study. Section III, deals with the fundamental field equations which allow then and the dynamical system. Finally, in section IV we conclude with our finding.

## II. THE MODEL

The Friedmann equation in which curvature is taken into account becomes given by

$$H^2 + \frac{k}{a^2} = \frac{\rho}{3}, \quad (1)$$

where the Hubble parameter  $H = \dot{a}/a$ , with  $a$  dot representing a derivative with respect to the cosmological time,  $a$  is the scale factor, and the curvature parameter  $k = 0, +1$ , and  $-1$  represents flat, closed and open spatial section, respectively. Here, we use units for which  $8\pi G = 1$ . The total energy density  $\rho$  is given by  $\rho = \rho_\phi + \rho_m$ , where  $\rho_\phi$  and  $\rho_m$  are the energy density of dark energy and dark matter, respectively. We will assume that these two components are conserve separately, satisfying the continuity equations

$$\dot{\rho}_m + 3H\rho_m = 0, \quad (2)$$

and

$$\dot{\rho}_\phi + 3H(\rho_\phi + p_\phi) = \dot{\rho}_\phi + 3H\rho_\phi(1 + w_\phi) = 0, \quad (3)$$

where  $w_\phi$  is the equation of state parameter introduced in the introduction.

We assume that the dark energy is modelled by a minimally-coupled scalar field  $\phi$ , where the pressure and density of the scalar field are given by

$$p_\phi = \frac{\dot{\phi}^2}{2} - V(\phi), \quad (4)$$

and

$$\rho_\phi = \frac{\dot{\phi}^2}{2} + V(\phi), \quad (5)$$

respectively. Here,  $V(\phi)$  represents the effective potential associated to the scalar field.

In term of the scalar field, Eq.(3) can be written as

$$\ddot{\phi} + 3H\dot{\phi} + V_{,\phi} = 0. \quad (6)$$

Equation (6) indicates that the field rolls down the hill in the scalar potential,  $V(\phi)$ , but its motion is damped by a term proportional to  $H$ .

### III. EVOLUTION WITH CURVATURE

We will assume that the scalar field moves in a nearly flat scalar potential,  $V(\phi)$ , quantitatively expressed as[27]

$$\left(\frac{1}{V} \frac{dV}{d\phi}\right)^2 \ll 1, \quad (7)$$

and

$$\frac{1}{V} \frac{d^2V}{d\phi^2} \ll 1. \quad (8)$$

The constraint given by Eq.(7) ensures that  $w_\phi \sim -1$ , meanwhile Eqs.(7) and (8) indicate that  $(1/V)(dV/d\phi)$  is nearly constant [27]. In the nomenclature of Ref.[22], these are thawing models, i.e.  $d\omega_\phi/d\phi > 0$ .

From the Friedmann equation we get

$$\Omega_k + \Omega_\phi + \Omega_m = 1,$$

where the density parameters are  $\Omega_\phi = \rho_\phi/(3H^2)$ ,  $\Omega_m = \rho_m/(3H^2)$  and  $\Omega_k = -k/(aH)^2$ , respectively.

Following, a similar technique developed in Ref.[27], Eqs.(1) and (6) can be expressed in terms of new variables  $x$ ,  $y$ ,  $\lambda$ , and  $\Omega_k$ , defined by

$$x = \phi'/\sqrt{6}, \quad (9)$$

$$y = \sqrt{V(\phi)/3H^2}, \quad (10)$$

$$\lambda = -V_{,\phi}/V, \quad (11)$$

$$\Omega_k = K/H^2, \quad (12)$$

where  $K \equiv -ka^{-2}$  and a prime denote the derivative with respect to  $\ln a$ , and  $V_{,\phi} = dV(\phi)/d\phi$ .

The density parameter  $\Omega_\phi$  is expressed in terms of the variables  $x^2$  and  $y^2$  in such a way that

$$\Omega_\phi = x^2 + y^2, \quad (13)$$

while, the equation of state parameter is given by

$$\gamma \equiv 1 + w_\phi = \frac{2x^2}{x^2 + y^2}. \quad (14)$$

Eqs.(1) and (6) can be written in terms of the new variables Eqs.(9)-(13), so that we get

$$x' = -3x + \lambda\sqrt{\frac{3}{2}}y^2 + \frac{3}{2}x \left[ 1 + x^2 - y^2 - \frac{\Omega_k}{3} \right], \quad (15)$$

$$y' = -\lambda\sqrt{\frac{3}{2}}xy + \frac{3}{2}y \left[ 1 + x^2 - y^2 - \frac{\Omega_k}{3} \right], \quad (16)$$

$$\lambda' = -\sqrt{6}\lambda^2(\Gamma - 1)x, \quad (17)$$

$$\Omega_k' = \Omega_k(1 - \Omega_k + 3[x^2 - y^2]), \quad (18)$$

where

$$\Gamma \equiv V \frac{d^2V}{d\phi^2} / \left( \frac{dV}{d\phi} \right)^2. \quad (19)$$

In the thawing model we have  $w_\phi \sim -1$  and thus the  $\gamma$  parameter satisfies  $\gamma = 1 + w_\phi \ll 1$ .

Therefore, it is useful to express Eqs.(15)- (18) in terms of  $\gamma$ ,  $\Omega_\phi$ ,  $\Omega_k$  and  $\lambda$ , respectively.

We obtain

$$\gamma' = -3\gamma(2 - \gamma) + \lambda(2 - \gamma)\sqrt{3\gamma\Omega_\phi}, \quad (20)$$

$$\Omega_\phi' = 3(1 - \gamma)\Omega_\phi(1 - \Omega_\phi) - \Omega_\phi\Omega_k, \quad (21)$$

$$\Omega_k' = \Omega_k(1 - \Omega_k + 3\Omega_\phi(\gamma - 1)) \quad (22)$$

$$\lambda' = -\sqrt{3}\lambda^2(\Gamma - 1)\sqrt{\gamma\Omega_\phi}. \quad (23)$$

At this point we would like to stress two assumptions that we are considering: the first is  $\gamma \ll 1$ , which corresponds to  $\omega_\phi \sim -1$ , as discussed previously. The second assumption we make is that the scalar field begins with an initial value in a potential which is nearly flat. In this way, following [27], we assume that  $\lambda$  is approximately constant, so that

$$\lambda \approx \lambda_0 = -(1/V)(dV/d\phi)\Big|_{\phi=\phi_0} \ll 1, \quad (24)$$

where  $\lambda_0$  is a small constant evaluated at  $\phi = \phi_0$ , the initial value of the scalar field which corresponds to when it starts to roll down the potential.

Let us first to consider the evolution of the system using initial values for the curvature  $\Omega_k = 0.005$ . The result is shown in figure 1. The same graph, but now with a value for the curvature  $\Omega_k = -0.005$  we get a similar plot with a small difference when compared with the previous case. The area in between the curves expands a continuous range of values of the

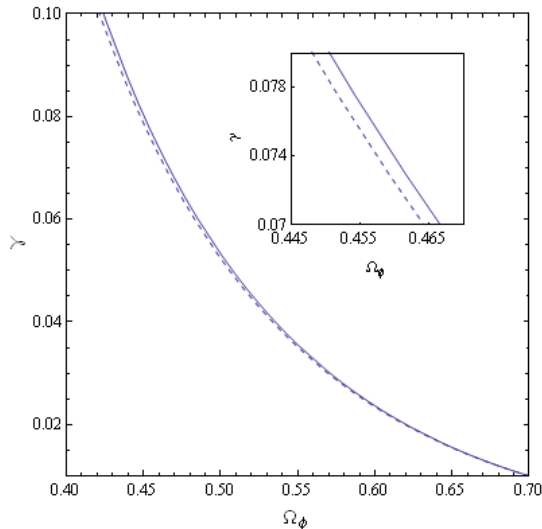


FIG. 1: Numerical results for  $\gamma$  as a function of the fractional density parameter  $\Omega_\phi$ , for nearly flat potentials. We have used the present values  $\Omega_{k0} = \pm 0.005$  and  $\Omega_{\phi 0} = 0.7$ , with  $\lambda_0 = 0.01$ .

curvature parameter, well inside the current observational constraints. In order to see this situation more clearly, we plot in figure 2 the projection of curves in the  $\Omega_k$ - $\Omega_\phi$  plane. We observe that a large region exist, even for small values  $\Omega_k$ . As a complement, in figure 3 we show the degeneracies in the variation of  $\gamma$  with respect to the curvature. All these figures are the result of a numerical integration of the system of Eqs. (20-23) with  $\lambda_0 = 0.01$ .

Motivated by the present value measured for the curvature parameter we make the assumption that the curvature is a small parameter, i.e.  $\Omega_k \ll 1$  along of the all story of the

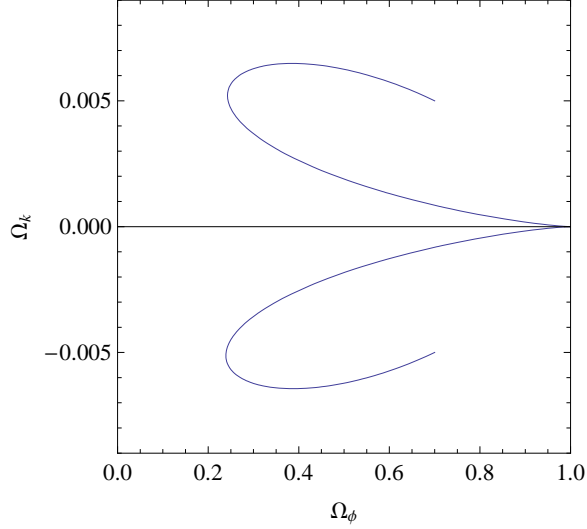


FIG. 2: Numerical results for  $\Omega_k$  as a function of the fractional density parameter  $\Omega_\phi$ , for nearly flat potentials. We have used the present values  $\Omega_{k0} = \pm 0.005$  and  $\Omega_{\phi0} = 0.7$ , with  $\lambda_0 = 0.01$ .

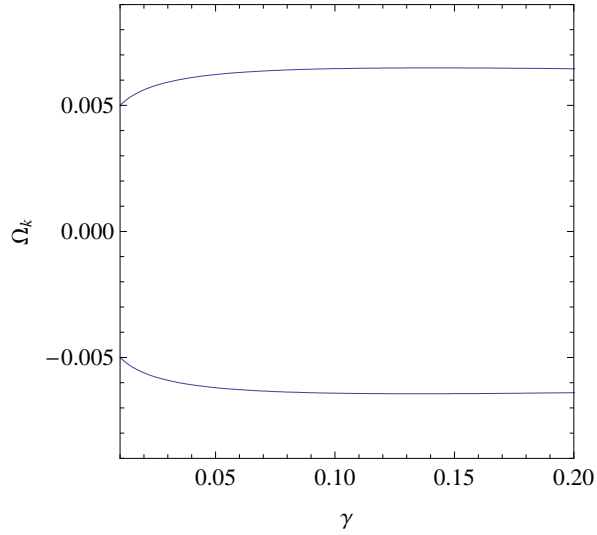


FIG. 3: Numerical results for  $\Omega_k$  as a function of  $\gamma$ , for nearly flat potentials. We have used the present values  $\Omega_{k0} = \pm 0.005$  and  $\Omega_{\phi0} = 0.7$ , with  $\lambda_0 = 0.01$ .

evolution of the universe. From Eqs. (20) and (21) we can write

$$\frac{d\gamma}{d\Omega_\phi} = \frac{-6\gamma + 2\lambda_0\sqrt{3\gamma\Omega_\phi}}{3\Omega_\phi(1 - \Omega_\phi)} + \frac{\lambda_0\Omega_k\sqrt{3\gamma\Omega_\phi}}{9\Omega_\phi(1 - \Omega_\phi)^2}, \quad (25)$$

where we have expanded and maintained the lowest order terms in  $\Omega_k$  and  $\gamma$ . Taking the

boundary value  $\gamma = 0$  at  $\Omega_\phi = 0$  (see Ref.[27]). The resulting solution is

$$\gamma = \frac{\lambda_0^2}{1296} \left[ \frac{12}{\sqrt{\Omega_\phi}} - \frac{\Omega_k(\Omega_\phi + 1)}{2(\Omega_\phi - 1)\sqrt{\Omega_\phi}} + F(\Omega_k, \Omega_\phi) \right]^2, \quad (26)$$

where

$$F(\Omega_k, \Omega_\phi) = \left( \frac{\Omega_\phi - 1}{\Omega_\phi} \right) \left( 12 + \frac{\Omega_k}{2} \right) \tanh^{-1} \sqrt{\Omega_\phi}. \quad (27)$$

Note that in the limit of a flat universe, i.e.,  $\Omega_k \rightarrow 0$ , we recover the expression given in Ref. [27].

In the same way we can derive an approximate solution from Eqs. (21) and (22) under the same approximations ( $\gamma \ll 1$  and  $\Omega_k \ll 1$ )

$$\frac{d\Omega_k}{d\Omega_\phi} = \frac{\Omega_k(1 - 3\Omega_\phi)}{3\Omega_\phi(1 - \Omega_\phi)}, \quad (28)$$

from which we get

$$\Omega_k = \Omega_{k0} \left[ \frac{1 - \Omega_\phi}{1 - \Omega_{\phi0}} \right]^{2/3} \left( \frac{\Omega_\phi}{\Omega_{\phi0}} \right)^{1/3}. \quad (29)$$

From Eqs.(26) and (29) we get

$$\gamma(\Omega_\phi) = \frac{\lambda_0^2}{1296} \left[ \frac{12}{\sqrt{\Omega_\phi}} - \frac{\Omega_{k0} \left[ \frac{1 - \Omega_\phi}{1 - \Omega_{\phi0}} \right]^{2/3} \left( \frac{\Omega_\phi}{\Omega_{\phi0}} \right)^{1/3} (\Omega_\phi + 1)}{2(\Omega_\phi - 1)\sqrt{\Omega_\phi}} + G(\Omega_\phi) \right]^2, \quad (30)$$

where the function  $G(\Omega_\phi)$  is given by

$$G(\Omega_\phi) = \left( \frac{\Omega_\phi - 1}{\Omega_\phi} \right) \left( 12 + \frac{\Omega_{k0} \left[ \frac{1 - \Omega_\phi}{1 - \Omega_{\phi0}} \right]^{2/3} \left( \frac{\Omega_\phi}{\Omega_{\phi0}} \right)^{1/3}}{2} \right) \tanh^{-1} \sqrt{\Omega_\phi}.$$

We can use equation (21) to solve for  $\Omega_\phi$  as a function of  $a$  and thus determine  $w_\phi(a)$ . Taking the limit  $\gamma \ll 1$  and  $\Omega_k \ll 1$  in equation (21) gives the following solution

$$\Omega_\phi = [1 + (\Omega_{\phi0}^{-1} - 1) a^{-3}]^{-1}, \quad (31)$$

where  $\Omega_{\phi0}$  and  $\Omega_{k0}$  are the present values of  $\Omega_\phi$ ,  $\Omega_k$ , respectively, and we take  $a = 1$  at present time. Combining Eq. (31) with Eq. (29) we obtain an approximated solution for  $\Omega_k(a)$ . Then, with the explicit expressions for  $\Omega_\phi(a)$  and  $\Omega_k(a)$ , and by using Eq. (26) we get explicitly the equation of state parameter  $w_\phi$ , as a function of the scale factor  $a$ , i.e.  $w_\phi(a)$ .



In Fig.(4) we show the dependence of the parameter  $w_\phi$  as a function of the scale factor  $a$ , for different values of the curvature parameter  $\Omega_k$  with  $w_0 = -0.95$  and  $\Omega_{\phi 0} = 0.7$ . Note that  $w_\phi(a)$  is not sensible to the value of  $\Omega_k = 0$  (see Ref.[27]).

We should mention that if we look for numerical solution to our set of dynamical Eqs., in which a scalar potential, such that  $V(\phi) \sim \phi^2, \phi^{-2}, \exp[-\phi]$ , etc, is used, we observe that there is no much changes when they are compared with that shown in Ref.[27], where  $\Omega_k = 0$  was taken into account.

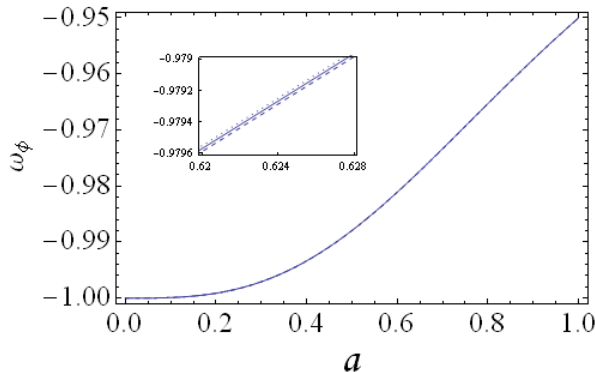


FIG. 4: Our anality results for the evolution of the parameter  $w_\phi$  as a function of the scale factor  $a$  for nearly flat potentials. Here, we have taken the values  $w_0 = -0.95$ ,  $\Omega_{\phi 0} = 0.7$ ,  $\Omega_{k0} = +0.005$  (dot line),  $\Omega_k = 0$  (solid line) and  $\Omega_k = -0.005$  (dash line), respectively.

Having an approximated expression for  $w_\phi(a)$  we can use it to perform a Bayesian analysis using SNIa observations, BAO distances and CMB shift parameter. In this work, we use the Supernova Cosmology Project Union sample [28], having 307 SN distributed over the range  $0.015 < z < 1.551$ . We fit the (theoretical) distance modulus  $\mu(z)_{th}$  defined by

$$\mu(z)_{th} = 5 \log_{10} \left[ \frac{H_0 d_L(z)}{c} \right] + \mu_0, \quad (32)$$

to the observational ones  $\mu(z)_{obs}$ . Here  $H_0 = 100 h \text{ km s}^{-1} \text{ Mpc}^{-1}$  is the Hubble constant and the luminosity distance is defined by  $d_L(z) = (1+z)r(z)$  where

$$r(z) = \frac{c}{H_0 \sqrt{|\Omega_k|}} \text{Sinn} \sqrt{|\Omega_k|} \int_0^z \frac{dz'}{H(z')}, \quad (33)$$

and  $\mu_0 = 42.38 - 5 \log_{10} h$ .  $\text{Sinn}(x) = \sin x, x, \sinh x$  for  $\Omega_k < 0, \Omega_k = 0$ , and  $\Omega_k > 0$  respectively. The second major input for parameter determination comes from the baryon acoustic oscillations (BAO) detected by Eisenstein et al. [29]. In our work, we add the

following term to the  $\chi^2$  of the model:

$$\chi_{BAO}^2 = \left[ \frac{(A - A_{BAO})}{\sigma_A} \right]^2, \quad (34)$$

where  $A$  is a distance parameter defined by

$$A = \frac{\sqrt{\Omega_m H_0^2}}{cz_{BAO}} \left[ r^2(z_{BAO}) \frac{cz_{BAO}}{H(z_{BAO})} \right]^{1/3}, \quad (35)$$

and  $A_{BAO} = 0.469$ ,  $\sigma_A = 0.017$ , and  $z_{BAO} = 0.35$ . The CMB shift parameter  $R$  is given by [30]

$$R(z_*) = \sqrt{\Omega_m H_0^2 r(z_*)}. \quad (36)$$

Here the redshift  $z_*$  (the decoupling epoch of photons) is obtained by using the fitting function [31]

$$z_* = 1048 \left[ 1 + 0.00124(\Omega_b h^2)^{-0.738} \right] \left[ 1 + g_1(\Omega_m h^2)^{g_2} \right], \quad (37)$$

where the functions  $g_1$  and  $g_2$  are given as

$$g_1 = 0.0783(\Omega_b h^2)^{-0.238} (1 + 39.5(\Omega_b h^2)^{0.763})^{-1}, \quad (38)$$

$$g_2 = 0.560 (1 + 21.1(\Omega_b h^2)^{1.81})^{-1}. \quad (39)$$

The WMAP-7 year CMB data alone yields  $R(z_*) = 1.726 \pm 0.018$  [32]. Defining the corresponding  $\chi_{CMB}^2$  as

$$\chi_{CMB}^2 = \frac{(R(z_*) - 1.726)^2}{0.018^2}, \quad (40)$$

one can deduce constraints on  $\Omega_{\phi 0}$ ,  $\omega_0$  and  $\Omega_{k0}$ . A joint analysis using SN+BAO+CMB leads to the best fit values showed in Fig.5, where we see the cross section of the  $\chi^2$  function in terms of the parameters  $\Omega_{\phi 0}$ ,  $\omega_0$  and  $\Omega_{k0}$ . The two horizontal lines indicate the 90% and 99% confidence range for each parameter.

The analysis shows that considering thawing quintessence with an explicit curvature term is consistent with observations. This is exactly the conclusion of [27] for the flat case in quintessence. However, as was demonstrated in [33], relaxing the slow-roll assumption, the equation of state parameter for different thawing potentials looks appreciably different. In the following, we consider both quintessence and Tachyon field models, and two scalar field potentials;  $V = \phi$  and  $V = \phi^{-2}$ . In figure ?? we show the integration of the field equations for current values of the curvature  $\Omega_{k0} = \pm 0.006$  and  $\Omega_{\phi 0} = 0.72$  for all the models. The potential are characterized by  $\Gamma = 0$  and  $\Gamma = 3/2$  respectively, along the initial

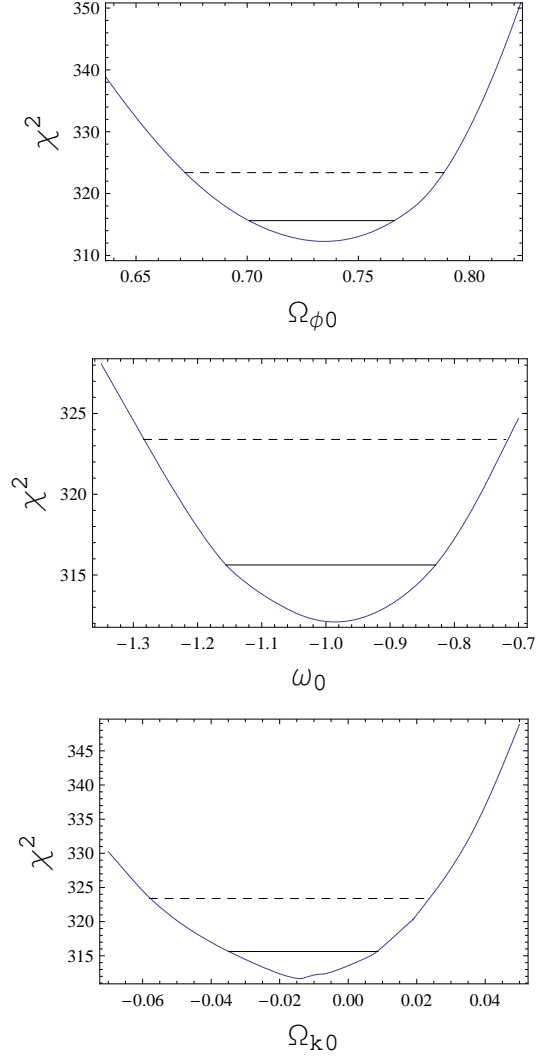


FIG. 5: This panel shows the  $\chi^2$  function computed using the approximate analytical solution of  $w_\phi(a)$ . The best fit parameters for  $\Omega_{\phi 0}$ ,  $\omega_0$  and  $\Omega_{k0}$ . The upper dashed line indicate the 99% confidence range for each parameter and the continuous line below indicate the 90% of confidence range for each parameter.

conditions  $\lambda_{ini} \simeq 1$  (assuming that the potential is not flat) and  $\gamma_{ini} \simeq 0$  (the equation of state parameter can vary from its freezing state ( $w = -1$ ) until today.)

#### IV. CONCLUSIONS

In the present work we have studied the thawing dark energy scenarios in which the effect of curvature was taking into account.

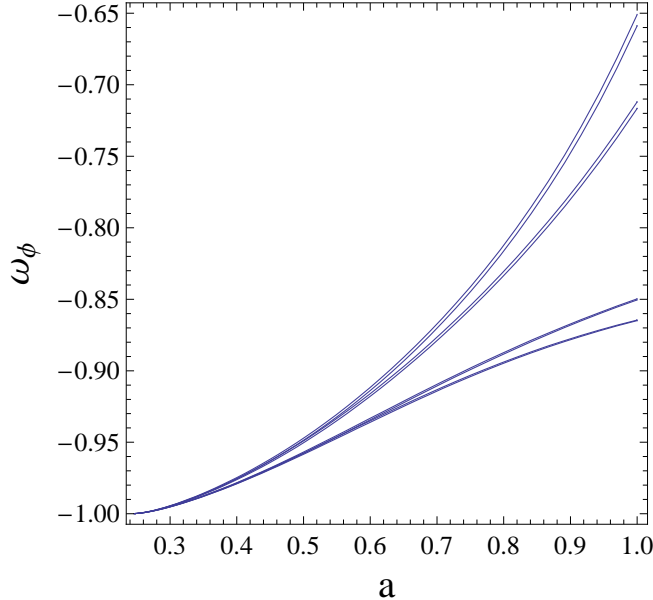


FIG. 6: Here we show the numerical integration for two scalar field models; quintessence and Tachyonic. We consider two scalar field potentials  $V = \phi$  and  $V = \phi^{-2}$  and in each case we use explicitly  $\Omega_{k0} = \pm 0.006$  with a current value  $\Omega_{\phi 0} = 0.72$ . The upper two curves correspond to a Tachyonic model with potential  $V = \phi$ . Although the values of the curvature parameter are very small, the separation of the curves increases with evolution and are appreciable here. The next couple of curves correspond to a quintessence scalar field model with potential  $V = \phi$ . The third set of two curves (which are closer each other than the previous ones) correspond to a Tachyonic model with potential  $V = \phi^{-2}$ . The bottom two curves correspond to a quintessence model with  $V = \phi^{-2}$ . All these models have  $\Omega_{\phi 0} = 0.72$ .

We have plotted numerically trajectories in the  $(\gamma, \Omega_\phi)$ ,  $(\Omega_k, \Omega_\phi)$  and  $(\Omega_k, \gamma)$  for a potential nearly flat.

We have shown that all such models converge to a common behavior and we have find the corresponding approximate analytical expressions for  $\gamma(\Omega_\phi)$  given by Eq.(30) and for  $w_\phi(a)$  in the cases when  $\gamma \ll 1$  and  $\Omega_k \ll 1$ . Here, we noted that an analitical solution for  $w_\phi(a)$  is not very perceptible to the value of  $\Omega_k \neq 0$ . A Bayesian analysis using SNIa data was performed to constraint the best fit parameters using our analytic function,  $w_\phi(a)$ . This analysis shows that current data does not rule out the model. In this way, the motivation is to see whether one can distinguish thawing dark energy models from  $\Omega_k \neq 0$  models using this method.

## Acknowledgments

This work was funded by Comision Nacional de Ciencias y Tecnología through FONDECYT Grants 1070306 (SdC) and 1090613 (RH and SdC), and by DI-PUCV Grant 123787 (SdC) and 123703 (RH).

---

- [1] M. Sullivan, *Lect. Note Phys.* **800**, 59 (2010).
- [2] A. G. Riess *et al*, *ApJ* **116**, 1009 (1998).
- [3] S. Perlmutter *et al*, *ApJ* **517**, 565 (1999).
- [4] D. Huterer and M. S. Turner, *Phys. Rev. D* **60**, 081301 (1999).
- [5] Sh. Tsujikawa, arXiv:1004.1493 [astro-ph. CO].
- [6] R. R. Caldwell, *Space. Sci. Rev.*, **148**, 347 (2009).
- [7] D.N. Spergel *et al*, *ApJ Suppl.* **148**, 175 (2003).
- [8] M. Tegmark *et al*, *Phys. Rev. D* **69**, 103501 (2004).
- [9] R. R. Caldwell, R. Dave and P. J. Steinhardt, *Phys. Rev. Lett.* **80**, 1582 (1998).
- [10] I. Zlatev, L. Wang and P. J. Steinhardt, *Phys. Rev. Lett.* **82**, 896 (1998).
- [11] T. Chiba, T. Okabe and M. Yamaguchi, *Phys. Rev. D* **62**, 023511 (2000).
- [12] C. Armendariz-Picon, V. F. Mukhanov and P. J. Steinhardt, *Phys. Rev. Lett.* **85** 4438 (2000).
- [13] C. Armendariz-Picon, V. F. Mukhanov and P. J. Steinhardt, *Phys. Rev. D* **63** 103510 (2001).
- [14] R. R. Caldwell, *Phys. Lett. B* **545**, 23 (2002).
- [15] S. M. Carroll, M. Hoffman and M. Trodden, *Phys. Rev. D* **68**, 023509 (2003).
- [16] S. D. H. Hsu, A. Jenkins and M. B. Wise, *Phys. Lett. B* **597**, 270 (2004).
- [17] X. Zhang, F. Q. Wu, *Phys. Rev. D* **76**, 023502 (2007).
- [18] H. Wei, S. N. Zhang, *Phys. Rev. D* **76**, 063003 (2007).
- [19] R. A. Daly, AIP Conf. Proc. **1166**, 81 (2009).
- [20] M. Sami, *Dark energy and possible alternatives.*, (2009) [arXiv:hep-th / 0901.0756].
- [21] C. Wetterich, *Nucl. Phys. B* **302**, 668 (1988); B. Ratra and P. J. E. Peebles, *Phys. Rev. D* **37** 3406 (1988); C. Armendariz-Picon, V. Mukhanov and P. J. Steinhardt, *Phys. Rev. Lett.* **85**, 4438 (2000); *idem* *Phys. Rev. D* **63**, 103510 (2001); T. Chiba, T. Okabe and M. Yamaguchi, *Phys. Rev. D* **62**, 023511 (2000).

- [22] R.R. Caldwell and E.V. Linder, *Phys. Rev. Lett.* **95**, 141301 (2005).
- [23] E.V. Linder, *Phys. Rev. D* **73**, 063010 (2006).
- [24] A. Guth, *Phys. Rev. D* **23**, 347 (1981).
- [25] D. Larson *et al*, arXiv:1001.4635 [astro-ph.CO].
- [26] E. Komatsu *et al*, arXiv:1001.4538v [astro-ph.CO].
- [27] R.J. Scherrer and A.A. Sen, *Phys. Rev. D* **77**, 083515 (2008).
- [28] M. Kowalski *et al*., *Astrophys. J.* 686, 749 (2008).
- [29] D. J. Eisenstein, *et al*, *Astrophys. J.* 633, 560 (2005).
- [30] J. R. Bond, G. Efstathiou, and M. Tegmark, *MNRAS* 291 L33(1997).
- [31] W. Hu, N. Sugiyama, *Astrophys. J.* 471, 542 (1996).
- [32] E. Komatsu, *et.al.*, [WMAP Collaboration], arXiv:1001.4538 [astro-ph.CO].
- [33] S. Sen, A.A. Sen and M. Sami, *Phys. Lett. B* **686**, 1 (2010), arXiv:0907.2814 [astro-ph.CO].